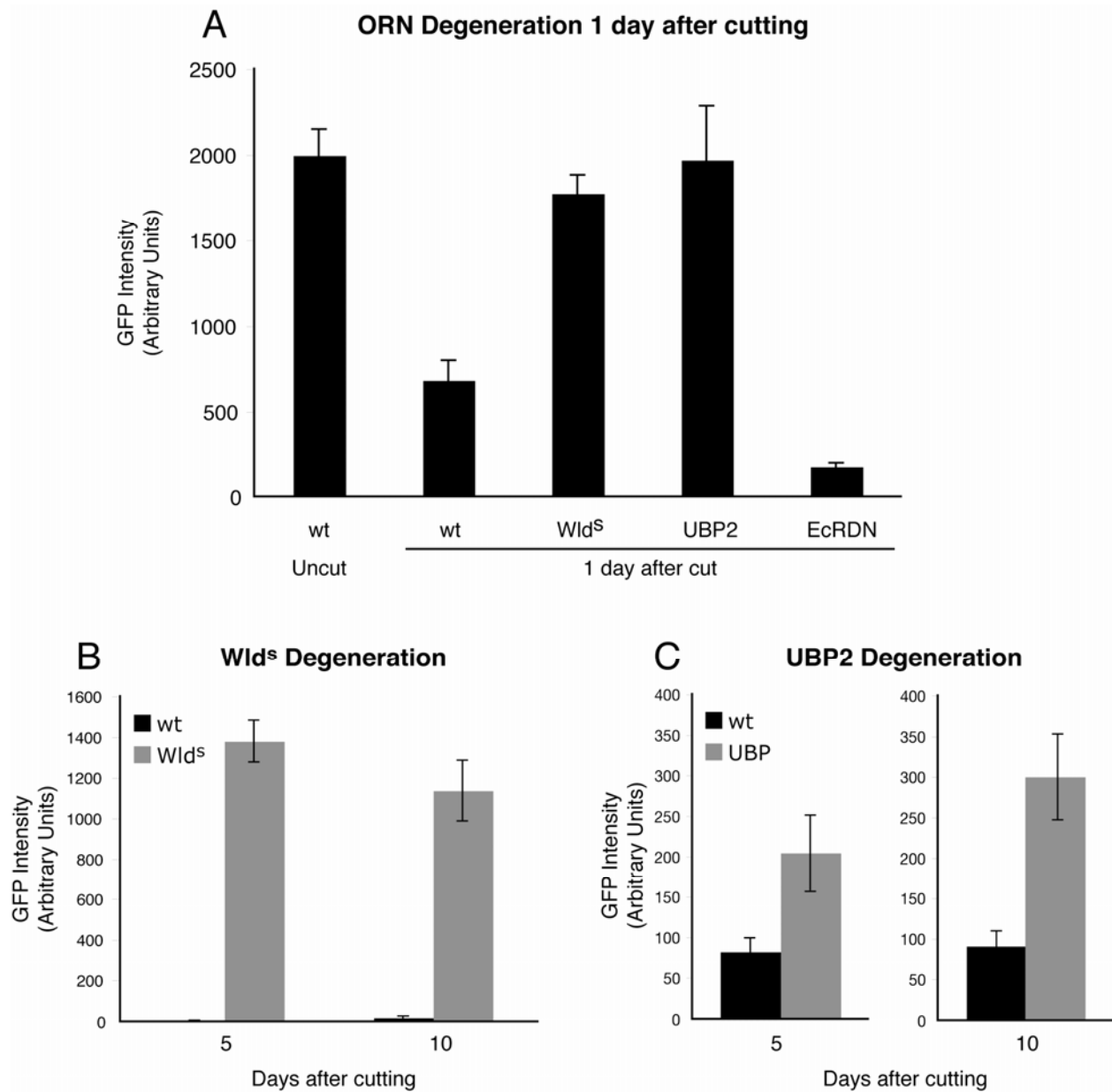


Supplemental Figure S1. Quantification of ORN axon degeneration



(A) Mean GFP intensity of commissural ORN axons 1 day after antennae removal. 1 day after cutting, wt ORNs show a significant decrease in GFP intensity at the commissure compared to wt uncut ORNs ( $p < 1 \times 10^{-4}$ ). By contrast, expression of either Wld<sup>S</sup> or UBP2 significantly delays

ORN degeneration 1 day after cutting ( $p=5 \times 10^{-4}$ ). ORNs expressing EcRDN show a significant decrease in GFP intensity even compared to wt cut axons ( $p=3 \times 10^{-4}$ ), and are undetectable at 5 and 10 days after antennae removal. Number of brains quantified: wt uncut (9), wt cut (10), Wld<sup>s</sup> cut (8), UBP2 cut (13), EcRDN cut (11).

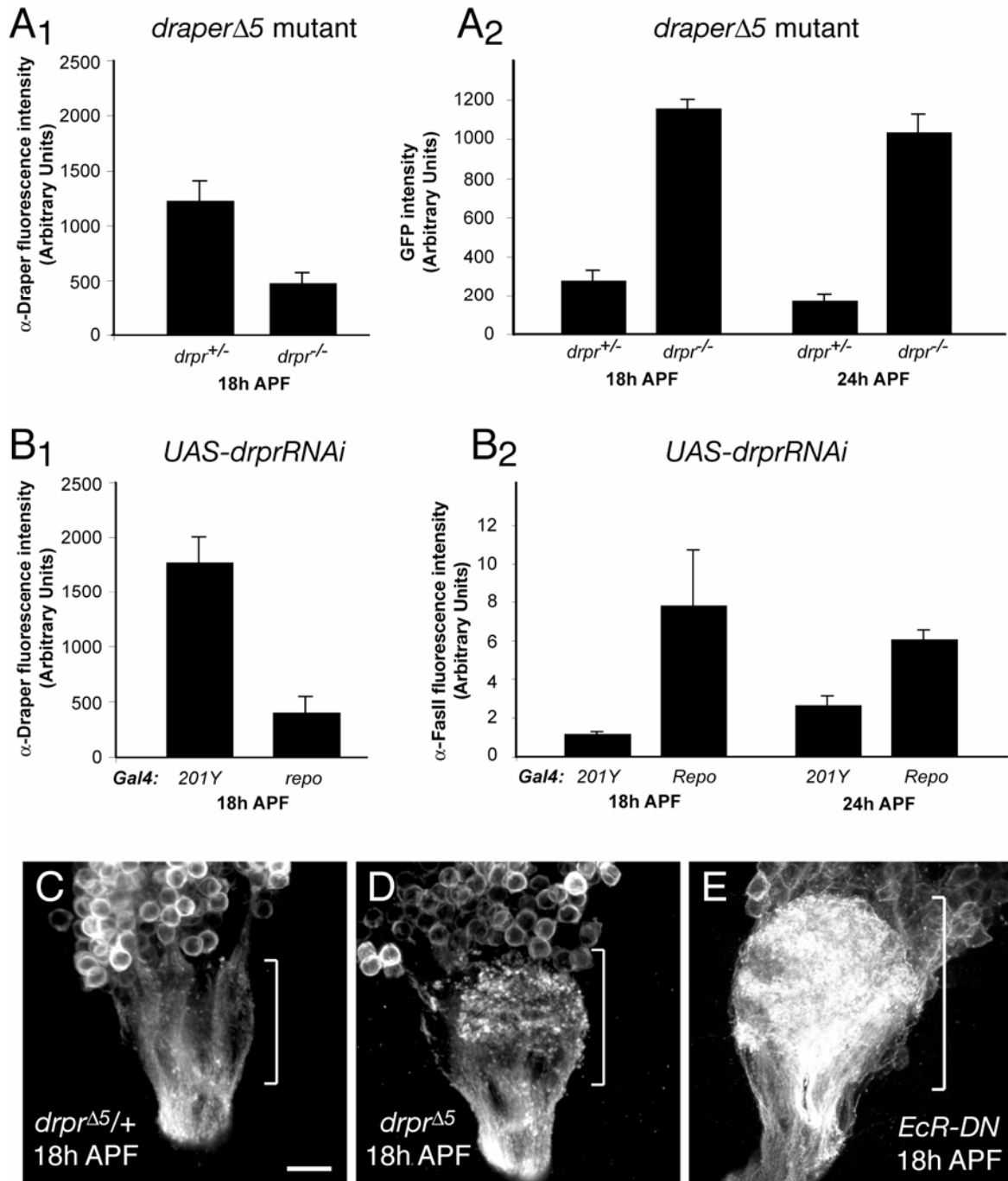
(B) Effect of Wld<sup>s</sup> expression on ORN degeneration at 5 and 10 days after antennae removal. Wld<sup>s</sup> significantly protects axons from degeneration at both 5 and 10 days after cutting as compared to wt ORNs whose commissural axons have completely degenerated ( $p < 1 \times 10^{-4}$ ). Number of brains quantified: 5 days after cut, wt (11), Wld<sup>s</sup> (8); 10 days after cut, wt (10), Wld<sup>s</sup> (10).

(C) Effect of UBP2 expression of ORN degeneration at 5 and 10 days after antennae removal. Compared to wt ORNs, UBP2 expression significantly delays ORN degeneration at both 5 days ( $p=0.016$ ) and 10 days ( $p < 1 \times 10^{-4}$ ) after cutting. However, it is notable that at these later time points the protective effect of UBP2 is less than that of Wld<sup>s</sup>, which strongly prevent ORN degeneration (compare Figures 4D<sub>3</sub> and 4F<sub>3</sub>). Number of brains quantified: 5 days after cut, wt (14), UBP2 (23); 10 days after cut, wt (13), UBP2 (23).

Error bars represent SEM.

Methods: Quantification was performed on confocal z-stacks of an equivalent number of optical slices that included the entire commissural axon bundle. For conditions compared directly in each graph images were taken using the same gain and background offset. However, due to the strong difference in intensity between Wld<sup>s</sup> and UBP2 axons at later time points, different image settings were used for Wld<sup>s</sup> and wt controls, and for UBP2 and wt controls. GFP intensity of axons was calculated by measuring the total GFP intensity of commissural axons between the two antennal lobes (i.e., not overlapping with nc82 staining) minus the background GFP intensity of an equivalent area just dorsal to the axon bundle. All p values were calculated by permutation test with 10,000 repetitions.

Supplemental Figure S2. Draper supplemental data



(A<sub>1</sub>) Quantification of Draper immunofluorescence intensity in dorsal lobes of *draper* heterozygous vs. homozygous animals at 18h APF. Homozygous *draper* mutants show a significant decrease in Draper staining intensity compared to heterozygous animals ( $p=7 \times 10^{-4}$ ,  $n=10$  and 8 MB dorsal lobes, respectively). The fluorescence intensity in homozygous *draper* likely represents background of antibody staining, as this allele is predicted to be a protein null.

(A<sub>2</sub>) Quantification of GFP intensity—as a measure of residual MB  $\gamma$  axons—in dorsal lobes of *draper* mutants at 18h and 24h APF. Homozygous mutants show significantly more GFP-labeled  $\gamma$  axons at both 18h and 24h APF than control flies (18h:  $p < 1 \times 10^{-4}$ ,  $n$  is same as A<sub>1</sub>; 24h:  $p = 5 \times 10^{-4}$ ,  $n=8$  MB dorsal lobes for both).

(B<sub>1</sub>) Quantification of Draper immunofluorescence intensity surrounding dorsal lobes at 18h APF with *draper* RNAi in glia (repo-Gal4) or  $\gamma$  neurons (201Y-Gal4). Knockdown of *draper* in glia results in a significant decrease in Draper staining intensity as compared to knockdown in  $\gamma$  neurons ( $p < 1 \times 10^{-4}$ ,  $n=8$  and 7 MB dorsal lobes, respectively).

(B<sub>2</sub>) Quantification of FasII intensity in dorsal lobes of *draper* RNAi flies at 18h and 24h APF. There are significantly more FasII-labeled axons in the dorsal lobes of glial-specific *draper* RNAi compared to  $\gamma$  neuron-specific knockdown at both 18h and 24h APF (18h:  $p < 1 \times 10^{-4}$ ,  $n$  is the same as B<sub>1</sub>; 24h:  $p=0.042$ ,  $n=7$  and 8 MB dorsal lobes, respectively).

(C) High-magnification views of MB calyx at 18h APF in *draper* heterozygous controls (same as in A) shows that the calyx (brackets) is devoid of GFP-labeled dendrite fragments ( $n=50$ ).

(D) In *draper* homozygous mutants, dendrites undergo fragmentation normally, but some dendritic fragments remain at 18h APF, long after they are normally cleared ( $n=12$ ).

(E) When pruning is inhibited by expression of EcR-DN in MB  $\gamma$  neurons, dendrites remain intact and no fragments are observed at 18h APF ( $n=10$ ).

Scale bar: 10  $\mu$ m. Error bars represent SEM. Genotypes: (C) and (D) are the same as Figure 7A and 7B, respectively; (E) *yw;FRT<sup>G13</sup>,UAS-mCD8::GFP,201Y-Gal4/+;UAS-EcR-W650A*.

Methods: In each experiment, brains from heterozygous and homozygous *draper* animals, or 201Y-Gal4 and Repo-Gal4 animals, were imaged at the same confocal settings. Quantification for GFP intensity and FasII intensity was performed on 10 $\mu$ m confocal z-stacks that included the

entire dorsal lobe of the MB. GFP,  $\alpha$ -Draper and  $\alpha$ -FasII fluorescence intensity was measured in an area surrounding the dorsal lobe equivalent to that shown in the insets for Figure 7A<sub>1</sub>. To normalize for differences in FasII intensity, dorsal lobe FasII intensity was calibrated against FasII intensity of the peduncle, which is not pruned. These comparisons underestimate the differences, because FasII-positive  $\alpha/\beta$  neurons invade dorsal lobes at 18h and more significantly at 24h APF under both conditions, and contribute to the total FasII intensity. Statistical analyses were performed as described in Figure S1.